Analog Integrated Circuits and Signal Processing (2021) 107:281–298
https://doi.org/10.1007/s10470-020-01751-5

Chaotic flower pollination algorithm based optimal PID controller design for a buck converter

Murat Erhan Çimen[1] · Zeynep B. Garip[2] · Ali Fuat Boz[1]

Received: 2 March 2020 / Revised: 9 September 2020 / Accepted: 11 November 2020 / Published online: 2 January 2021

Abstract
This paper presents a solution based on optimal PID coefficients including anti-wind up for buck converter presents using meta-heuristic algorithm and chaos theory. A hybrid algorithm is called chaotic based flower pollination algorithm is provided by combining flower pollination algorithm and chaos theory with different maps. Five different choatic maps are used in the aim of increasing the efficacy and efficiency of flower pollination algorithm. In order to adjust the parameters combined in the flower pollination algorithm, random number sequences from Henon, Logistic, Sine, Tent and Tinkerbell chaotic maps are used. The success of the developed algorithm is evaluated by solving 23 different benchmark problems which are very common in the literature. The results of comparative experiments show that henon chaotic map based flower pollination algorithm is sufficiently effective in solving these benchmark problems. Thus desinging optimal PID with anti-windup for buck converter, henon chaotic map based flower pollination algorithm is used. Also henon chaotic map based flower pollination algorithm has better performance than firelfy algorithm and whale optimization algorithm existing in literature.

Keywords Flower pollination algorithm · Chaotic maps · PID design · Buck Converter

1 Introduction

DC-DC converters are one of the basic power electronics circuits that convert the electrical voltage level to another level using the switching feature. These converters are widely used in many fields such as power supplies, portable industrial mobile devices, electric vehicles due to their high efficiency, power density, power levels, low cost and small size [1, 2].

Meta-heuristic algorithms are often inspired by complex biological events and nonlinear behaviors in nature such as flashing patterns of fireflies, fish and bird schooling in nature, ants communication with pheromone, predatory behaviors of the wolves, foraging behavior of honey bees. These nonlinear behaviors are associated with the deterministic chaos theory [3, 4]. The most important feature of meta-heuristic algorithms is trying to find the most suitable solution by randomly searching the search space to solve a problem. Similarly, the maps produced by chaotic systems contain randomness [5, 6]. Also, using these chaotic maps in optimization algorithms can increase the performance of optimization algorithms. While the improvement of the performance of these algorithms has been confirmed by statistical and experimental studies, it has not been proven mathematically yet [7–9]. Genetic Algorithm (GA), Harmonic Algorithm, Particle Swarm Optimization (PSO), Artificial Bee Colony (ABC), Firefly (FA), Ant Colony Optimizayion, Food Foragining Optimization Algorithm (BFOA) have been conducted to improve the performance of algorithms using chaos theory [10–15].

Adjusting PID controller parameter is one of the major problems in improving performance and efficiency in the design of DC-DC converters. The PID operation needs to

✉ Zeynep B. Garip
zbatik@subu.edu.tr

Murat Erhan Çimen
muratcimen@subu.edu.tr

Ali Fuat Boz
afboz@subu.edu.tr

[1] Electrical and Electronic Engineering Department, Sakarya University of Applied Sciences, 54050 Serdivan, Sakarya, Turkey

[2] Computer Engineering Department, Sakarya University of Applied Sciences, 54050 Serdivan, Sakarya, Turkey

get feedback from the output of the system to regulate the system at desired performance. While conventional methods such as Ziegler-Nichols, Cohen-Coon, Chien-Hrones-Reswick, fuzzy logic have been used to adjust PID controller parameters [16–19], meta-heuristic algorithms have recently been used by researchers [20–23]

In this study, meta-heuristic algorithm was used to find optimal PID coefficients in a Buck converter. A hybrid algorithm is called chaotic based flower pollination algorithm is provided by combining flower pollination algorithm and chaos theory. The success of the developed algorithm is evaluated by solving 23 different benchmark problems which are very common in the literature. As a result, the PID controller designed with the henon chaotic map based flower pollution algorithm for the Buck converter was compared with the whale optimization and firefly algorithms in the literature.

2 Mathematical model of buck converter

Buck converters are widely used to reduce high voltage to a lower voltage level efficiently. V_{DC} is an input voltage. V_0 is generated by using switching through this V_{DC} voltage. Thus, a lower voltage is provided thanks to V_{DC}. Switching is performed at high frequency [24, 25]. This high frequency rectangular waveform signal is formed by inductor (L) and capacitor (C) like a low pass filter. C, shown in Fig. 1, is used to reduce the fluctuation in the output voltage [21]. In some cases, the combination of the inductor and the capacitor is used to reduce the fluctuation in the load. In some cases, the capacitor combination is used with the inductor to reduce the fluctuation in the load.

In Fig. 1, V_{DC} = Supply voltage, V_D = Voltage through the diode, V_L = Voltage through the inductor, V_C = Voltage through the Capacitor, V_O = Output Voltage of the Buck converter. The transistor is used as the switching element in the buck convertor [25, 26]. Therefore, the circuit works in two cases according to the state of the switch being on or off [26]. Vo is controlled by changing the on-off $(t_{open} - t_{close})$ time of the switching step. This value, which is called the switching ratio (d) and determines the value of the output voltage, is calculated using Eq. 1. The sum of the open and closed switching times gives the switching period, ie $T = t_{open} - t_{close}$.

$$V_0 = dV_{DC}, \quad d = \frac{t_{on}}{T} \tag{1}$$

The mathematical model of the system changes according to the state of the switches. When the key is open, the states of the system are as in Eq. 2. Equation will be as in 3 when the key is closed [26, 27].

$$\textit{Switch} \quad \textit{on}: \quad \underbrace{\begin{bmatrix} \dot{i_L} \\ \dot{V_C} \end{bmatrix}}_{\dot{x}} = \underbrace{\begin{bmatrix} \dfrac{\left[-R_L + \dfrac{R_C R_{Load}}{R_{Load}+R_C}\right]}{L} & \dfrac{-R_{Load}}{L(R_{Load}+R_C)} \\ \dfrac{R_{Load}}{C(R_{Load}+R_C)} & \dfrac{-1}{C(R_{Load}+R_C)} \end{bmatrix}}_{A_1} \underbrace{\begin{bmatrix} i_L \\ V_C \end{bmatrix}}_{x} + \underbrace{\begin{bmatrix} \frac{1}{L} \\ 0 \end{bmatrix}}_{B_1} \underbrace{V_{DC}}_{u} \tag{2}$$

$$\textit{Switch} \quad \textit{off}: \quad \underbrace{\begin{bmatrix} \dot{i_L} \\ \dot{V_C} \end{bmatrix}}_{\dot{x}} = \underbrace{\begin{bmatrix} \dfrac{\left[-R_{Load} + \dfrac{R_C R_{Load}}{R_{Load}+R_C}\right]}{L} & \dfrac{-R_{Load}}{L(R_{Load}+R_C))} \\ \dfrac{R_{Load}}{C(R_{Load}+R_C))} & \dfrac{-1}{C(R_{Load}+R_C))} \end{bmatrix}}_{A_2} \underbrace{\begin{bmatrix} i_L \\ V_C \end{bmatrix}}_{x} + \underbrace{\begin{bmatrix} 0 \\ 0 \end{bmatrix}}_{B_2} \underbrace{V_{DC}}_{u} \tag{3}$$

In order to show the on and off times effect of the switches by using Eqs. 2 and 3, the mean values of the state equations are obtained in Eq. 4.

$$\underbrace{\begin{bmatrix} \dot{i_L} \\ \dot{V_C} \end{bmatrix}}_{\dot{x}} = \underbrace{[dA_1 + (1-d)A_2]}_{A} \underbrace{\begin{bmatrix} i_L \\ V_C \end{bmatrix}}_{x} + \underbrace{[dB_1 + (1-d)B_2]}_{B} \underbrace{V_{DC}}_{u} \tag{4}$$

The parameters of buck converter used in this study are given in Table 1.

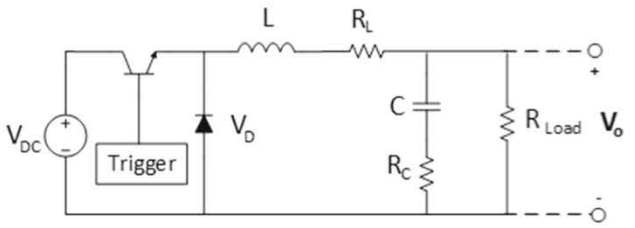

Fig. 1 Buck Converter

3 Development of chaotic based flower pollution algorithm

3.1 Chaotic maps

Chaos and random numbers represent unpredictable irregular behaviors as well as being deterministic. Meta-heuristic algorithms, similar to the chaos order, were inspired by the disorder of the biological system [5]. Small changes in the initial values of the chaotic cause large changes in system behavior. In this study, frequently applied are discrete chaotic maps are used. The formulation of the different chaotic maps used in this study are given in Table 2. Chaotic maps visulations are given in Fig. 2.

3.2 Flower pollination algorithm

The Flower Pollination Algorithm (FPA), developed by Yang [28, 29], is a meta-heuristic algorithm imitating the pollination process of flowering plants. Flower pollination is a process associated with the transfer of flower pollen. The main actors of this transfer are birds, bats, insects and other animals. There are some flowers and insects that do what we call a flower pollinator partnership. These flowers can only attract birds involved in this partnership. These insects are considered as the main pollinator for the flowers [29, 30].

In FPA, four different rules of the feature of the pollination process, pollination behavior and flower constancy are considered.

- Rule 1: Biotic pollination is a cross-pollination process in which pollen is carried by the pollinator. This is a global pollination process and the movement of pollinators matches the Lévy flights.
- Rule 2: Abiotic or self-pollination is the process of the same plant or flower without pollinator. This process is known as local pollination because the pollen carrying distance is usually shorter than biotic pollination.
- Rule 3: Pollinators can improve flower stability, which tends to certain types of flowers. The flower constant is equivalent to the probability of reproduction. This probability is proportional to the similarity of the associated flowers.
- Rule 4: The possibility of a key; $p \in [0, 1]$ is used to control the pollination type. According to these rules, two different search techniques (local and global) can be used. The best solutions can be found among the existing ones by applying local search. In addition, global pollination essentially prevents trapping in a local optimum solution.

These rules need to be transformed into updated equations. For example, in the global pollination stage, flower pollen gametes are carried by pollinators such as insects. Pollen can travel over long distances because insects can often fly and move over a much longer area. Therefore, Rule 1 and flower constancy (Rule 3) can be represented mathematically by Eq. 5.

$$x_i^{t+1} = x_i^t + \gamma L(\lambda)(g^* - x_i^t)) \tag{5}$$

Here x_i^t is i_{th} solution vector in t_{th} iteration and g^* is the best solution among the all solutions in the current iteration. Here γ is a scaling factor to control the step size.

Basically L(λ) is the Lévy flight step size parameter. The movement of the insects can be shown according to the Lévy distribution while they are travelling long distances. Lévy's mathematical expression is shown in Eq. 6.

$$L \sim \frac{\lambda \Gamma(\frac{\lambda\pi}{2})}{\pi} \frac{1}{s^{1+\lambda}} \quad (s \gg s_0 > 0) \tag{6}$$

Here, $\Gamma(\lambda)$ is the standard gamma function and s is the step size. This distribution applies to larger steps $s > 0$. In theory, $s_0 \gg 0$ is required, but in practice s_0 can be as small as 0.1. For local pollination, both Rule 2 and Rule 3 are shown in Eq. 7.

$$x_i^{t+1} = x_i^t + \varepsilon(x_j^t - x_k^t) \tag{7}$$

In Eq. 7, x_j^t, x_k^t are two rondamly selected dolutions and $\varepsilon \in [0, 1]$ that are pollen species from different flowers of the same plants. The most important feature of this algorithm for optimization is to search many solution points in search space by using Levy distribution. Determination of solution points at long distances by biotic pollination model as in flowers and researching the neighborhood of solution points with abiotic pollination model constitute the optimization logic of the algorithm.

Table 1 Buck Converter Parameters

Parameters	Value
R_L	140 Ω
R_C	0.28 mΩ
C	2200 Ω
L	0.3 mH
R_{Load}	100 Ω
V_{DC}	100 V

Algorithm 1 The so-called code of FPA algorithm

Objective function f(**x**), $\mathbf{x}(x_1, x_2, .., x_n)^T$
Generate a random initial population. (n: Pollen number)
Calculate the best solution for the initial population g^*
Probability key $p \in [0, 1]$
while t < maximum iteration number **do**
  for i=1:n **do**
    if rand <p **then**
      Global pollination $x_i^{t+1} = x_i^t + \gamma L(\lambda)(g^* - x_i^t))$
    else
      Local pollination $x_i^{t+1} = x_i^t +$ rand $\times (g^* - x_i^t)$
    end if
    Evaluate new solutions.
    Update better solutions in the population
  end for
  Choose the best solution g^*
end while

3.3 Developed chaotic based FPA algorithm

Chaotic based methods replace the random generators available in many applications as they increase the stochastic search capability [7]. Therefore, developed Chaotic-FPA algorithm is obtained by changing the rand and epsilon parameters in the structure with chaotic map functions. The values of the rand and epsilon variables in the equation are logistic, tent, henon, sinus, tinkerbell chaotic map based functions taking values within the range [0,1]. The so-called code of the Chaotic-FPA algorithm obtained by developing the FPA algorithm is given in Algorithm 2. The so-called code of the FPA algorithm is given in Algorithm 1 and develop Chaotic FPA Algorithm is given in Algorithm 2.

Table 2 Buck Converter Parameters

Name	Chaotic map equation	Parameters
Logistic	$x_{i+1} = \alpha x_i(1 - x_i)$	α=3.9 $x_0 = 0.5$
Tent	$x_{i+1} = f(x_i, \mu)$ $f(x_i, \mu) = \begin{cases} f_L(x_i, \mu) = \mu x_i & x_i < 0.5 \\ f_R(x_i, \mu) = \mu(1 - x_i) & x_i \geq 0.5 \end{cases}$	$\mu = 1.41$ $x_0 = 0.1$
Henon	$x_{i+1} = 1 - \alpha x_i^2 + by_i$ $y_{i+1} = x_i$	$\alpha = 1.4$ $b = 0.3$ $x_0 = 0$ $x_1 = 0$
Sin	$x_{i+1} = rsin(\pi x_i)$	$r = 0.867$ $x_0 = 0.5$
Tinkerbell	$x_{i+1} = x_i^2 - y_i^2 + \alpha x_i + by_i$ $y_{i+1} = 2x_i y_i + cx_i + dy_i$	$\alpha = 0.9$ $b = -0.6013$ $c = 2.0$ $d = 0.5$ $x_0 = -0.72$ $y_0 = -0.64$

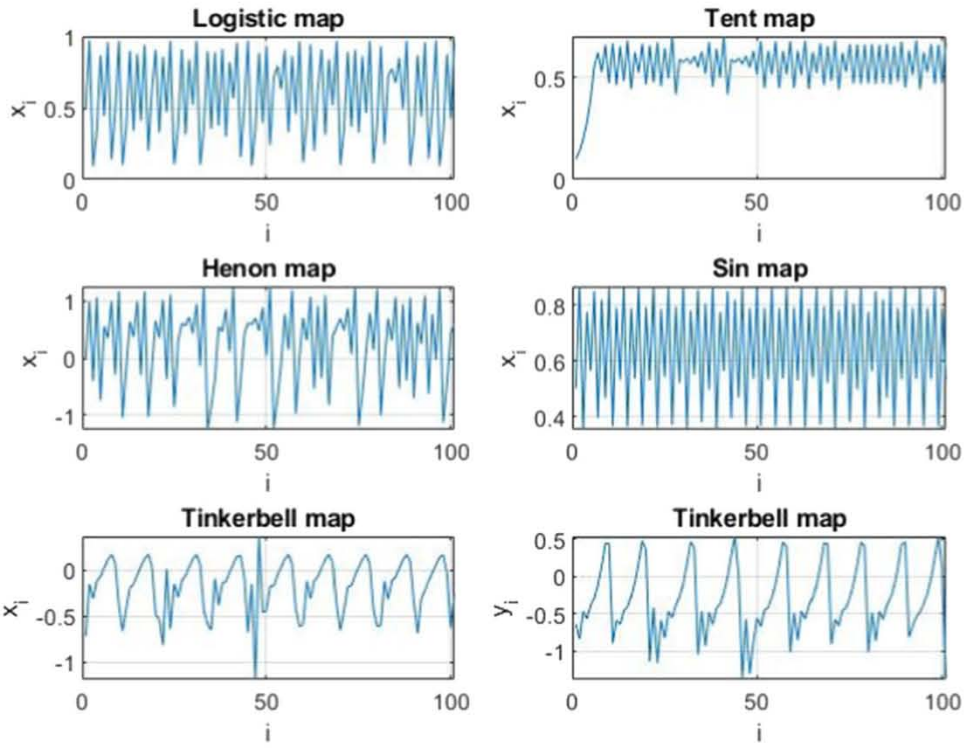

Fig. 2 Chaotic Maps Visulation

Algorithm 2 The so-called code of the developed chaotic-FPA algorithm

Objective function f(**x**), $\mathbf{x}(x_1, x_2, .., x_n)^T$
Generate a random initial population. (n: Pollen number)
Calculate the best solution for the initial population g^*
Probability key $p \in [0, 1]$
while t < maximum iteration number **do**
  for i=1:n **do**
    if r(Chaotic map) <p **then**
      Global pollination $x_i^{t+1} = x_i^t + \gamma L(\lambda)(g^* - x_i^t))$
    else
      Local pollination $x_i^{t+1} = x_i^t +$ r(Chaotic Map)$(g^* - x_i^t))$
    end if
    Evaluate new solutions.
    Update better solutions in the population
  end for
  Choose the best solution g^*
end while

3.4 Comparison of orginal FPA and chaotic based FPA performances

In order to compare the success of the proposed algorithm, there are benchmark functions which are difficult to solve in the literature. These problems were solved in order to measure the performance of the algorithm developed with the proposed chaotic maps. Table 3 presents the benchmark functions from F1 to F23.

Simulation studies were performed on a computer with Intel (R) Core (TM) i5-3470 CPU @ 3.20 Ghz, 64 Bit, 8GB RAM in Windows 10 operating system to solve benchmark functions. In order to see the effect of chaotic behavior added to the algorithm in FPA, 3 different configurations were arranged. These configurations show the parameter values that the algorithm run on. These parameter values are given in Table 4. Generally, swarm size and number of iterations were changed. Depending on the parameters in the configuration, each problem was run 100 times under equal conditions. The original FPA and chaotic FPA results are evaluated statistically and given in between Table 5,

Table 3 Benchmark Functions employed in our experimental study

Functions	Variable Number	Value Range	F_{min}
Category I: unimodal benchmark functions			
$F_1 = \sum_{i=1}^{n} x_i^2$	30	[− 100,100]	0
$F_2 = \sum_{i=1}^{n} \lvert x_i \rvert + \prod_{i=1}^{n} \lvert x_i \rvert$	30	[− 10,10]	0
$F_3 = \sum_{i=1}^{n} \left(\sum_{j=1}^{i} (x_j) \right)^2$	30	[− 100,100]	0
$F_4 = max\{ \lvert x_i \rvert, 1 \le i \le n \}$	30	[− 30,30]	0
$F_5 = \sum_{i=1}^{n-1} \left[100 \left(x_{i+1} - x_2^i \right)^2 + (x_i - 1)^2 \right]$	30	[− 30,30]	0
$F_6 = \sum_{i=1}^{n} [x_i + 0.5]^2$	30	[− 30 30]	0
$F_7 = \sum_{i=1}^{n} i x_i^4 + random(0,1)$	30	[− 1.28,1.28]	0
Category II: multimodal benchmark functions			
$F_8 = \sum_{i=1}^{n} -x_i sin\left(\sqrt{\lvert x_i \rvert} \right)$	30	[− 500,500]	− 418.9829x5
$F_9 = \sum_{i=1}^{n} \left[x_i^2 - 10cos(2\pi) x_i + 10 \right]$	30	[− 5.12,5.12]	0
$F_{10} = -20exp\left(-0.2\sqrt{\frac{1}{n}\sum_{i=1}^{n} x_i^2} \right) - exp\left(-0.2\sqrt{\frac{1}{n}\sum_{i=1}^{n} cos(2\pi x_i)} \right) + 20 + e$	30	[− 32,32]	0
$F_{11} = \frac{1}{4000}\sum_{i=1}^{n} x_i^2 - \prod_{i=1}^{n} cos\left(\frac{x_i}{\sqrt{i}} \right) + 1$	30	[− 600,600]	0
$F_{12} = \frac{\pi}{n} \left\{ \begin{array}{c} 10sin(\pi y_i) + \\ \sum_{i=1}^{n-1} (x_i + 0.5)^2 [1 + 10sin^2(\pi y_{i+1})] \\ + (y_n - 1)^2 \end{array} \right\} + \sum_{i=1}^{n-1} u(x_i, 10, 100, 4)$, $y_i = 1 + \frac{x_i + 1}{4}$, $u(x_i, 10, 100, 4) = \begin{cases} k(x_i - a)^m & x_i > a \\ 0 & -a \le x_i \le a \\ k(-x_i - a)^m & x_i < -a \end{cases}$	30	[− 50,50]	0
$F_{13} = 0.1 \left\{ \begin{array}{c} sin^2(3\pi x_1) + \\ \sum_{i=1}^{n} (x_i - 1)^2 [1 + sin^2(3\pi + x_i)] \\ + (x_n - 1)^2 [1 + sin^2(2\pi x_n)] \end{array} \right\} + \sum_{i=1}^{n-1} u(x_i, 10, 100, 4)$, $u(x_i, 10, 100, 4) = \begin{cases} k(x_i - a)^m & x_i > a \\ 0 & -a \le x_i \le a \\ k(-x_i - a)^m & x_i < -a \end{cases}$	30	[− 50,50]	0
Functions	Variable Number	Value Range	F_{min}
Category III: fix dimension multimodal benchmark functions			
$F_{14} = \left(\frac{1}{500} + \sum_{j=1}^{25} \frac{1}{j + \sum_{i=1}^{2} \left(x_i - a_{ij} \right)^2} \right) - 1$	2	[− 65,65]	1
$F_{15} = \sum_{i=1}^{11} \left[a_i - \frac{x_1 \left(b_i^2 + b_i x_2 \right)}{b_i^2 + b_i x_3^3 + x_4} \right]^2$	4	[− 5,5]	0.00030
$F_{16} = 4x_1^2 - 2.1x_1^4 + \frac{1}{3}x_1^6 + x_1 x_2 - 4x_2^2 + 4x_2^4$	2	[− 5,5]	− 1.0316
$F_{17} = \left(x_1 - \frac{5.1}{4\pi^2}x_1^2 + \frac{5}{\pi}x_1 - 6 \right)^2 + 10\left(1 - \frac{1}{8\pi} \right) cos(x_1) + 10$	2	[− 5,5]	0.398
$F_{18} = \left[1 + (x_1 + x_2 + 1)^2 (19 - 14x_1 + 3x_1^2 - 14x_2 + 6x_1 x_2 + 3x_2^2) \right] \times \left[30 + (2x_1 - 3x_2)^2 \right.$	2	[− 2,2]	3

Table 3 (continued)

Functions	Variable Number	Value Range	F_{min}
$\times\left(18-32x_1+12x_1^2+48x_2-36x_1x_2+32x_2^2\right)]$			
$F_{19}=-\sum_{i=1}^{4} c_i exp\left(-\sum_{j=1}^{3} a_{ij}\left(x_j-p_{ij}\right)^2\right)$	3	[1,3]	− 3.86
$F_{20}=-\sum_{i=1}^{4} c_i exp\left(-\sum_{j=1}^{6} a_{ij}\left(x_j-p_{ij}\right)^2\right)$	6	[0,1]	− 10.1532
$F_{21}=-\sum_{i=1}^{5}\left[(X-a_i)(X-a_i)^T+c_i\right]^{-1}$	5	[0,10]	− 10.1532
$F_{22}=-\sum_{i=1}^{7}\left[(X-a_i)(X-a_i)^T+c_i\right]^{-1}$	7	[0,10]	− 10.4028
$F_{23}=-\sum_{i=1}^{10}\left[(X-a_i)(X-a_i)^T+c_i\right]^{-1}$	10	[0,10]	− 10.5363

Table 4 Flower Pollution Algorithm Parameters for Configuration 1, Configuration 2 and Configuration 3

Parameter name	Parameter value
Configuration 1: result of F1-23 benchmark functions	
Population size	100
Probabilty switch	0.8
Iteration number	100
Configuration 2: result of F1-23 benchmark functions	
Population size	100
Probabilty switch	0.8
Iteration number	2000
Configuration 3: result of F1-23 benchmark functions	
Population size	100
Probabilty switch	0.8
Iteration number	2500

Tables 6 and 7. These data include minimum value, maximum value, expected value and standard deviations produced by algorithms according to functions and using FPA and chaotic FPA. Looking at these data, maximums, minimums and expected value are required to be close to the desired value, while standard deviation is required to be close to zero for global success. For this purpose, tables are arranged according to the relevant configuration and determined maps of the algorithms. Table 8 shows how many times the algorithm receives the best minimum value, best maximum value, best expected value and best standard deviation values within these valuables.

The parameters given in configuration 1 are commonly used in the literature. The statistical data obtained by FPA and chaotic FPA algorithms according to each function when the algorithm is run according to these parameters are given in Table 4. In this analysis made according to Configuration 1, again based on this Table 5, the minimum, maximum, expected value and standard deviation are given in Table 5.

When the algorithm is run according to these parameters, statistical data obtained by FPA and chaotic FPA algorithms for each function are given in Table 5. In these analyses according to configuration 1, it is given in Table 8 that how many times the algorithm gives the best results in minimum, maximum, expected value and standard deviation compared to the others based on the Table 5.

The parameters given in Configuration 2 are chosen differently from the literature in order to produce the desired result of the algorithm and thus increase its success. When the algorithm is run according to these parameters given in Table 4, statistical data obtained by FPA and chaotic FPA algorithms according to each function are given in Table 6. In these analyses according to configuration 2, it is given in Table 8 that how many times the algorithm gives the best result in minimum, maximum, expected value and standard deviation compared to the others based on this Table 6.

The parameters given in the configuration 3 are chosen differently from the values in the literature in order to produce the desired result for the algorithm and thus increase its success. When the algorithm is run according to these parameters given in Table 4, statistical data obtained by FPA and chaotic FPA algorithms for each function are given in Table 7. In these analyses according to Configuration 3, it is given in Table 8 that how many times the algorithm gives the best result in minimum, maximum, expected value and standard deviation compared to others based on Table 7.

Table 8 summarizes the results given in Tables 5, 6 and 7. Table 8 shows how many best results are available in Tables 5, 6 and 7. When the average values are examined, the Henon map performed better compared to

Table 5 Configuration 1: Result of F1-F23 benchmark functions

		Orginal	Henon map	Logistic map	Sine map	Tent map	Tinkerbell map
Category I: Unimodal benchmark functions							
F1	Ort	2,05E+00	2,27E+00	2,96E+04	4,16E+04	4,07E+04	3,51E+04
	Max	3,05E+00	2,27E+02	4,02E+04	4,75E+04	4,70E+04	4,75E+04
	Min	8,37E-01	0,00E+00	2,13E+04	3,07E+04	3,09E+04	1,76E+04
	Std	3,71E-01	2,27E+01	3,54E+03	3,07E+03	2,65E+03	7,13E+03
F2	Ort	8,26E+03	2,35E+03	9,80E+03	5,42E+05	2,59E+05	6,53E+06
	Max	2,06E+05	8,97E+04	2,72E+05	2,92E+07	4,72E+06	1,48E+08
	Min	9,31E+01	5,71E+01	8,75E+01	1,23E+02	1,79E+02	6,90E+01
	Std	2,47E+04	9,38E+03	3,21E+04	3,12E+06	6,80E+05	1,86E+07
F3	Ort	3,80E+04	3,03E+04	3,73E+04	5,21E+04	5,20E+04	4,33E+04
	Max	5,44E+04	4,67E+04	5,11E+04	6,65E+04	6,79E+04	6,32E+04
	Min	2,48E+04	1,61E+04	2,08E+04	4,16E+04	4,15E+04	2,02E+04
	Std	5,40E+03	5,75E+03	6,11E+03	5,60E+03	5,37E+03	8,42E+03
F4	Ort	6,49E+01	6,14E+01	6,50E+01	7,15E+01	7,17E+01	7,15E+01
	Max	7,08E+01	7,12E+01	7,26E+01	7,70E+01	7,62E+01	8,23E+01
	Min	5,08E+01	4,33E+01	5,57E+01	6,33E+01	6,36E+01	6,09E+01
	Std	4,14E+00	5,10E+00	3,22E+00	2,32E+00	2,13E+00	5,16E+00
F5	Ort	5,20E+07	3,46E+07	4,88E+07	8,99E+07	8,89E+07	8,14E+07
	Max	7,77E+07	6,93E+07	7,37E+07	1,15E+08	1,15E+08	1,74E+08
	Min	2,41E+07	1,23E+07	1,83E+07	5,91E+07	5,65E+07	2,14E+07
	Std	9,99E+06	1,24E+07	1,13E+07	1,04E+07	1,01E+07	2,79E+07
F6	Ort	2,85E+04	2,27E+04	2,84E+04	4,19E+04	4,10E+04	3,55E+04
	Max	3,68E+04	3,28E+04	3,63E+04	4,69E+04	4,71E+04	4,98E+04
	Min	1,73E+04	1,18E+04	1,87E+04	3,44E+04	3,31E+04	1,75E+04
	Std	3,82E+03	4,06E+03	3,68E+03	2,51E+03	2,64E+03	6,37E+03
F7	Ort	2,37E+01	1,67E+01	2,30E+01	4,42E+01	4,36E+01	3,61E+01
	Max	3,61E+01	3,40E+01	3,40E+01	5,37E+01	5,73E+01	6,29E+01
	Min	9,87E+00	4,22E+00	6,68E+00	3,03E+01	2,79E+01	4,10E+00
	Std	5,49E+00	5,99E+00	5,15E+00	5,25E+00	5,65E+00	1,18E+01
Category II: Multimodal benchmark functions							
F8	Ort	−5,90E+03	−5,71E+03	−5,91E+03	−6,01E+03	−6,02E+03	−4,26E+03
	Max	−5,49E+03	−5,17E+03	−5,42E+03	−5,35E+03	−5,40E+03	−3,44E+03
	Min	−6,64E+03	−6,46E+03	−6,47E+03	−6,53E+03	−6,57E+03	−5,47E+03
	Std	2,23E+02	2,27E+02	2,21E+02	2,21E+02	2,47E+02	3,48E+02
F9	Ort	2,69E+02	2,75E+02	2,66E+02	2,64E+02	2,64E+02	3,50E+02
	Max	2,95E+02	3,12E+02	2,95E+02	2,91E+02	2,90E+02	3,94E+02
	Min	2,44E+02	2,33E+02	2,39E+02	2,34E+02	2,37E+02	2,80E+02
	Std	1,22E+01	1,50E+01	1,18E+01	1,28E+01	1,20E+01	2,31E+01
F10	Ort	1,97E+01	1,91E+01	1,98E+01	2,00E+01	2,00E+01	1,96E+01
	Max	2,02E+01	2,00E+01	2,02E+01	2,03E+01	2,02E+01	2,03E+01
	Min	1,85E+01	1,73E+01	1,89E+01	1,96E+01	1,96E+01	1,76E+01
	Std	2,98E-01	5,60E-01	2,67E-01	1,20E-01	1,34E-01	4,78E-01
F11	Ort	2,64E+02	2,01E+02	2,61E+02	3,75E+02	3,71E+02	3,27E+02
	Max	3,38E+02	2,87E+02	3,32E+02	4,28E+02	4,34E+02	4,64E+02
	Min	1,97E+02	1,03E+02	1,46E+02	3,16E+02	2,91E+02	1,38E+02
	Std	3,19E+01	4,11E+01	3,27E+01	2,13E+01	2,62E+01	6,92E+01

Table 5 (continued)

		Orginal	Henon map	Logistic map	Sine map	Tent map	Tinkerbell map
F12	Ort	6,02E+07	3,67E+07	5,70E+07	1,35E+08	1,29E+08	1,33E+08
	Max	1,01E+08	1,04E+08	1,13E+08	1,85E+08	1,86E+08	3,02E+08
	Min	9,94E+06	4,54E+06	9,55E+06	7,24E+07	6,70E+07	1,20E+07
	Std	1,78E+07	2,05E+07	1,91E+07	2,15E+07	2,66E+07	6,83E+07
F13	Ort	1,72E+08	1,07E+08	1,69E+08	3,45E+08	3,37E+08	3,25E+08
	Max	2,97E+08	2,61E+08	2,75E+08	5,07E+08	4,39E+08	6,21E+08
	Min	5,02E+07	2,63E+07	4,18E+07	2,33E+08	2,32E+08	7,52E+07
	Std	5,42E+07	4,55E+07	4,63E+07	4,98E+07	4,26E+07	1,38E+08
Category III: Fix Dimension Multimodal benchmark functions							
F14	Ort	1,07E+00	1,18E+00	1,29E+00	2,74E+00	2,56E+00	1,24E+00
	Max	2,82E+00	3,14E+00	3,63E+00	5,78E+00	5,59E+00	3,07E+00
	Min	9,98E−01	9,98E−01	9,98E−01	9,99E−01	9,98E-01	9,98E−01
	Std	2,33E−01	3,45E−01	4,63E-01	1,19E+00	1,24E+00	4,35E−01
F15	Ort	2,89E−03	1,46E−03	3,13E−03	1,88E−02	1,81E−02	2,32E−03
	Max	7,67E−03	2,29E−03	1,02E−02	6,34E−02	6,43E−02	7,03E−03
	Min	9,71E−04	7,28E−04	9,45E−04	2,21E−03	1,20E−03	8,74E−04
	Std	1,52E−03	3,30E−04	1,87E−03	1,15E−02	1,29E−02	1,14E−03
F16	Ort	−1,03E+00	−1,03E+00	−1,03E+00	−8,98E-01	−9,22E−01	−1,03E+00
	Max	−1,02E+00	−1,03E+00	−1,02E+00	−2,54E-01	−1,70E−01	−1,02E+00
	Min	−1,03E+00	−1,03E+00	−1,03E+00	−1,03E+00	−1,03E+00	−1,03E+00
	Std	1,39E−03	1,80E−04	1,93E−03	1,52E−01	1,43E−01	2,68E−03
F17	Ort	3,98E−01	3,98E−01	3,98E−01	3,98E−01	3,98E−01	4,00E−01
	Max	3,98E−01	3,98E−01	3,98E−01	3,99E−01	3,99E−01	4,11E−01
	Min	3,98E−01	3,98E−01	3,98E−01	3,98E−01	3,98E−01	3,98E−01
	Std	7,78E−05	5,38E−05	8,42E−05	1,99E−04	1,48E−04	2,57E−03
F18	Ort	3,12E+00	3,02E+00	3,13E+00	1,13E+01	1,12E+01	3,05E+00
	Max	7,72E+00	3,09E+00	5,08E+00	3,21E+01	3,20E+01	3,59E+00
	Min	3,00E+00	3,00E+00	3,00E+00	3,12E+00	3,20E+00	3,00E+00
	Std	4,76E-01	1,52E-02	2,24E-01	6,35E+00	7,23E+00	7,39E-02
F19	Ort	−3,86E+00	−3,86E+00	−3,85E+00	−3,74E+00	−3,75E+00	−3,86E+00
	Max	− 3,83E+00	− 3,86E+00	− 3,82E+00	− 3,56E+00	− 3,51E+00	− 3,83E+00
	Min	− 3,86E+00	− 3,86E+00	− 3,86E+00	− 3,86E+00	− 3,86E+00	− 3,86E+00
	Std	4,65E-03	1,47E-03	6,81E-03	7,25E-02	7,48E-02	5,33E− 03
F20	Ort	− 3,16E+00	− 3,18E+00	− 3,16E+00	− 2,78E+00	− 2,81E+00	− 3,07E+00
	Max	− 2,80E+00	− 3,06E+00	− 2,93E+00	− 2,19E+00	− 2,36E+00	− 2,78E+00
	Min	− 3,28E+00	− 3,29E+00	− 3,29E+00	− 3,15E+00	− 3,15E+00	− 3,25E+00
	Std	7,00E-02	4,29E-02	7,05E-02	2,49E-01	1,87E-01	8,29E-02
F21	Ort	− 6,70E+00	− 6,58E+00	− 6,10E+00	− 4,04E+00	− 3,89E+00	− 5,84E+00
	Max	− 4,38E+00	− 4,86E+00	− 4,00E+00	− 9,98E− 01	− 1,05E+00	− 4,13E+00
	Min	− 9,88E+00	− 1,00E+01	− 9,27E+00	− 7,99E+00	− 7,39E+00	− 9,98E+00
	Std	1,39E+00	1,26E+00	1,15E+00	1,57E+00	1,54E+00	1,32E+00
F22	Ort	− 6,31E+00	− 6,33E+00	− 6,11E+00	− 3,91E+00	− 4,01E+00	− 4,87E+00
	Max	− 3,49E+00	− 4,58E+00	− 3,58E+00	− 1,33E+00	− 1,15E+00	− 2,57E+00
	Min	− 9,51E+00	− 1,00E+01	− 8,95E+00	− 8,57E+00	− 8,42E+00	− 9,10E+00
	Std	1,29E+00	1,19E+00	1,25E+00	1,56E+00	1,57E+00	1,21E+00

Table 5 (continued)

		Orginal	Henon map	Logistic map	Sine map	Tent map	Tinkerbell map
F23	Ort	− 6,74E+00	− 6,36E+00	− − 6,20E+00	− 3,82E+00	− 4,24E+00	− 4,55E+00
	Max	− 3,60E+00	− 4,26E+00	− 3,37E+00	− 1,66E+00	− 1,87E+00	− 2,38E+00
	Min	− 1,02E+01	− 9,75E+00	− 9,59E+00	− 6,60E+00	− 8,49E+00	− 1,00E+01
	Std	1,61E+00	1,28E+00	1,44E+00	1,26E+00	1,40E+00	1,52E+00

the results from other maps. Additionally, in terms of maximum, minimum and standard deviation values, henon map based FPA gave the best results. Henon map is the most successful when the success of the algorithms is evaluated over average and it is followed by the Original FPA and Logistic map based FPA. Other chaotic map based algorithm which gives the worst values in terms of average, maximum and minimum performance criteria and therefore shows the least success. This indicates that the algorithm is converged to local minimum. According to comparison results for configuration 1, configuration 2 and configuration 3, Henon map based FPA performed better than Original FPA, Logistic map, Sine map, Tinkerbell map and Tent chaotic map based algorithms.

In general, the FPA Algorithm with Henon Map was more successful than the other maps and the one with orginal FPA.

4 Application of PID controller to buck converter system using chaotic based flower pollination algorithm

In order to adjust the Buck converter output voltage, it is desired that the output voltage be equalized to the reference value by providing a comparison with the Vref value. Therefore, an appropriate compensator is required for the system. The Error = Vref-Vo value occurs when this arrangement is provided.

In this study, PID controller is used as a regulator to prevent the change between input voltage and output voltage. The PID controller contains three separate parameters. These are; Proportional Value (P) determining the effect of the existing error, Integral (I) determining the effect based on the sum of the final errors, and Derivative (D) determining the effect given the rate of change of the error.

The block diagram of buck converter with PID controller, determined with Henon Based Chaotic-FPA, is shown in Fig. 3. In this study, anti-wind up technique called clamping was also applied in order to avoid integral winding. There are multiple error calculation criteria when calculating the parameters of the PID controller. Generally, performance criteria such as integral of absolute error (IAE), integral squared error (ISE), Integral Time Absolute Error (ITAE) and integral of Time Multiplied Square Error (ITSE) are used in algorithms. In order to compare this study with previous studies in the literature, ISE fitness function was chosen as the error criterion. In addition, the aim of this study was to minimize the ISE error and to achieve the desired 10% overshoot limit. The objective function in Eq. 8 is used for this.

$$\begin{aligned} &FitneesFunction \\ &min(ISE) \qquad \int E(t)^2 dt \\ &Subjectto \qquad V_0 < V_{0max} \end{aligned} \tag{8}$$

The parameters of Buck converter used in the developed Henon Based Chaotic-FPA are given in Table 9. The control signal of the system given in Fig. 3 varies between 0-1 u_{trig}. Exceeding this range results in a constant value being generated by the comparison operator. In order to solve this problem, saturation value is added to the controller and anti-wind up feature is added.

4.1 Experimental results and discussion

Simulation studies were carried out in which anti-wind up feature was considered. The success of the algorithm according to the desired objective function is listed in Table 10. According to these results, the low standard deviation indicates that the result has consistently reached the same value. In other words, the proposed algorithm provides fitness to the global solution every time.

Table 11 also includes the results of the Buck converter obtained with the developed Henon Based Chaotic-FPA, the results of the studies found in the literature and ISE error values, which are the performance criteria. In addi-

Table 6 Configuration 2: Result of F1-F23 benchmark functions

		Orginal	Henon map	Logistic map	Sine map	Tent map	Tinkerbell map
Category I: unimodal benchmark functions							
F1	Ort	3,28E-01	1,08E+00	2,80E-01	5,78E+00	5,63E+00	9,91E+02
	Max	4,92E-01	1,42E+00	3,83E-01	7,23E+00	7,00E+00	1,72E+03
	Min	2,16E-01	5,62E-01	2,16E-01	4,23E+00	3,99E+00	4,53E+02
	Std	8,26E-02	2,34E-01	5,62E-02	8,68E-01	9,05E-01	3,32E+02
F2	Ort	2,24E+01	8,75E+00	1,75E+01	5,66E+01	4,12E+01	5,39E+01
	Max	5,12E+01	2,10E+01	7,12E+01	1,08E+02	1,11E+02	8,48E+01
	Min	8,43E+00	4,40E+00	7,69E+00	7,80E+00	1,26E+01	2,66E+01
	Std	1,15E+01	3,98E+00	1,42E+01	3,67E+01	2,58E+01	1,39E+01
F3	Ort	9,79E+00	1,37E+01	1,32E+01	1,50E+03	1,10E+03	1,16E+03
	Max	1,39E+01	1,99E+01	1,84E+01	1,87E+03	1,42E+03	1,98E+03
	Min	7,67E+00	1,05E+01	7,70E+00	1,31E+03	7,22E+02	7,58E+02
	Std	1,72E+00	3,16E+00	2,69E+00	1,45E+02	2,26E+02	3,65E+02
F4	Ort	1,72E+01	9,15E+00	1,64E+01	2,39E+01	2,38E+01	3,33E+01
	Max	1,95E+01	1,13E+01	1,95E+01	2,63E+01	2,58E+01	3,81E+01
	Min	1,49E+01	6,65E+00	1,30E+01	2,21E+01	2,17E+01	2,42E+01
	Std	1,29E+00	1,17E+00	1,84E+00	1,29E+00	1,25E+00	3,75E+00
F5	Ort	9,88E+01	1,36E+02	9,38E+01	2,40E+02	2,22E+02	1,58E+05
	Max	1,27E+02	1,96E+02	1,23E+02	3,25E+02	2,73E+02	2,98E+05
	Min	6,40E+01	8,97E+01	6,64E+01	1,88E+02	1,77E+02	6,46E+04
	Std	1,51E+01	2,47E+01	1,67E+01	3,99E+01	2,42E+01	6,29E+04
F6	Ort	3,40E-01	1,06E+00	2,70E-01	5,81E+00	5,41E+00	9,01E+02
	Max	5,19E-01	1,73E+00	3,66E-01	7,87E+00	8,05E+00	1,73E+03
	Min	1,82E-01	7,60E-01	1,83E-01	3,47E+00	3,89E+00	4,38E+02
	Std	7,96E-02	2,41E-01	5,08E-02	1,14E+00	1,05E+00	2,97E+02
F7	Ort	1,39E-01	4,28E-02	1,52E-01	8,14E-01	7,35E-01	4,74E-01
	Max	2,01E-01	6,68E-02	2,33E-01	9,47E-01	8,72E-01	6,69E-01
	Min	8,93E-02	1,29E-02	8,37E-02	6,91E-01	4,53E-01	2,03E-01
	Std	2,99E-02	1,36E-02	4,05E-02	7,83E-02	1,08E-01	1,41E-01
Category II: Multimodal benchmark functions							
F8	Ort	-8,64E+03	-8,80E+03	-8,69E+03	-8,80E+03	-8,77E+03	-7,51E+03
	Max	-8,41E+03	-8,49E+03	-8,30E+03	-8,51E+03	-8,47E+03	-6,96E+03
	Min	-9,06E+03	-9,36E+03	-9,01E+03	-9,58E+03	-9,10E+03	-1,02E+04
	Std	1,54E+02	2,00E+02	2,08E+02	2,30E+02	1,70E+02	7,99E+02
F9	Ort	1,18E+02	9,61E+01	1,15E+02	1,12E+02	1,08E+02	1,79E+02
	Max	1,32E+02	1,13E+02	1,28E+02	1,25E+02	1,26E+02	2,16E+02
	Min	1,05E+02	7,13E+01	1,02E+02	8,78E+01	9,31E+01	1,46E+02
	Std	7,33E+00	1,14E+01	6,92E+00	1,02E+01	8,97E+00	1,92E+01
F10	Ort	1,22E+01	4,35E+00	1,25E+01	1,95E+01	1,91E+01	8,46E+00
	Max	1,66E+01	6,56E+00	1,60E+01	1,98E+01	1,97E+01	1,11E+01
	Min	9,02E+00	1,77E+00	9,76E+00	1,91E+01	1,76E+01	6,68E+00
	Std	1,98E+00	1,11E+00	1,82E+00	2,07E-01	6,21E-01	1,33E+00
F11	Ort	4,22E-01	8,22E-01	3,87E-01	1,05E+00	1,05E+00	9,40E+00
	Max	5,10E-01	9,32E-01	4,64E-01	1,07E+00	1,07E+00	1,24E+01
	Min	3,33E-01	7,45E-01	2,89E-01	1,04E+00	1,04E+00	5,31E+00
	Std	4,27E-02	5,33E-02	4,22E-02	9,10E-03	9,14E-03	2,25E+00

Table 6 (continued)

		Orginal	Henon map	Logistic map	Sine map	Tent map	Tinkerbell map
Category I: unimodal benchmark functions							
F12	Ort	4,93E+00	1,74E+00	5,14E+00	6,17E+00	6,18E+00	1,41E+02
	Max	5,93E+00	2,58E+00	6,04E+00	8,42E+00	6,98E+00	1,81E+03
	Min	4,26E+00	9,85E-01	4,06E+00	5,38E+00	5,53E+00	2,15E+01
	Std	4,26E-01	4,50E-01	4,77E-01	6,49E-01	4,43E-01	3,94E+02
F13	Ort	6,66E+00	3,89E+00	6,33E+00	2,43E+01	2,43E+01	5,54E+04
	Max	9,55E+00	6,67E+00	9,52E+00	2,84E+01	2,75E+01	3,19E+05
	Min	3,91E+00	1,65E+00	2,14E+00	1,86E+01	1,48E+01	4,74E+03
	Std	1,57E+00	1,40E+00	1,94E+00	2,48E+00	3,00E+00	7,31E+04
Category III: Fix Dimension Multimodal benchmark functions							
F14	Ort	9,98E-01	9,98E-01	9,98E-01	9,98E-01	9,98E-01	9,98E-01
	Max	9,98E-01	9,98E-01	9,98E-01	9,98E-01	9,98E-01	9,98E-01
	Min	9,98E-01	9,98E-01	9,98E-01	9,98E-01	9,98E-01	9,98E-01
	Std	1,92E-11	1,84E-16	1,15E-12	1,31E-05	1,30E-11	3,87E-10
F15	Ort	3,57E-04	3,07E-04	3,66E-04	6,66E-04	6,66E-04	5,21E-04
	Max	5,49E-04	3,07E-04	5,68E-04	1,07E-03	7,59E-04	6,57E-04
	Min	3,10E-04	3,07E-04	3,09E-04	5,02E-04	4,69E-04	3,31E-04
	Std	5,62E-05	3,08E-10	6,77E-05	1,26E-04	8,32E-05	9,76E-05
F16	Ort	-1,03E+00	-1,03E+00	-1,03E+00	-1,03E+00	-1,03E+00	-1,03E+00
	Max	-1,03E+00	-1,03E+00	-1,03E+00	-1,03E+00	-1,03E+00	-1,03E+00
	Min	-1,03E+00	-1,03E+00	-1,03E+00	-1,03E+00	-1,03E+00	-1,03E+00
	Std	9,04E-15	8,82E-17	1,35E-14	2,74E-12	1,85E-11	3,89E-08
F17	Ort	3,98E-01	3,98E-01	3,98E-01	3,98E-01	3,98E-01	3,98E-01
	Max	3,98E-01	3,98E-01	3,98E-01	3,98E-01	3,98E-01	3,98E-01
	Min	3,98E-01	3,98E-01	3,98E-01	3,98E-01	3,98E-01	3,98E-01
	Std	1,37E-14	2,38E-15	3,69E-15	8,92E-11	3,07E-13	8,56E-07
F18	Ort	3,00E+00	3,00E+00	3,00E+00	3,00E+00	3,00E+00	3,00E+00
	Max	3,00E+00	3,00E+00	3,00E+00	3,00E+00	3,00E+00	3,00E+00
	Min	3,00E+00	3,00E+00	3,00E+00	3,00E+00	3,00E+00	3,00E+00
	Std	8,62E-14	7,49E-16	2,88E-13	3,51E-09	3,88E-09	1,14E-07
F19	Ort	-3,86E+00	-3,86E+00	-3,86E+00	-3,86E+00	-3,86E+00	-3,86E+00
	Max	-3,86E+00	-3,86E+00	-3,86E+00	-3,86E+00	-3,86E+00	-3,86E+00
	Min	-3,86E+00	-3,86E+00	-3,86E+00	-3,86E+00	-3,86E+00	-3,86E+00
	Std	3,94E-13	2,28E-15	2,76E-13	4,68E-09	1,16E-09	2,43E-07
F20	Ort	-3,32E+00	-3,32E+00	-3,32E+00	-3,32E+00	-3,32E+00	-3,32E+00
	Max	-3,32E+00	-3,32E+00	-3,32E+00	-3,32E+00	-3,32E+00	-3,30E+00
	Min	-3,32E+00	-3,32E+00	-3,32E+00	-3,32E+00	-3,32E+00	-3,32E+00
	Std	3,37E-10	1,64E-09	6,30E-10	5,24E-07	8,69E-08	4,63E-03
F21	Ort	-1,02E+01	-1,02E+01	-1,02E+01	-1,02E+01	-1,02E+01	-1,02E+01
	Max	-1,02E+01	-1,02E+01	-1,02E+01	-1,02E+01	-1,02E+01	-1,02E+01
	Min	-1,02E+01	-1,02E+01	-1,02E+01	-1,02E+01	-1,02E+01	-1,02E+01
	Std	1,80E-08	2,89E-11	3,88E-08	1,14E-06	8,57E-07	1,63E-04
F22	Ort	-1,04E+01	-1,04E+01	-1,04E+01	-1,04E+01	-1,04E+01	-1,04E+01
	Max	-1,04E+01	-1,04E+01	-1,04E+01	-1,04E+01	-1,04E+01	-1,04E+01
	Min	-1,04E+01	-1,04E+01	-1,04E+01	-1,04E+01	-1,04E+01	-1,04E+01
	Std	2,62E-08	3,48E-11	2,13E-08	1,26E-06	1,37E-06	3,07E-04
F23	Ort	-1,05E+01	-1,05E+01	-1,05E+01	-1,05E+01	-1,05E+01	-1,05E+01
	Max	-1,05E+01	-1,05E+01	-1,05E+01	-1,05E+01	-1,05E+01	-1,05E+01
	Min	-1,05E+01	-1,05E+01	-1,05E+01	-1,05E+01	-1,05E+01	-1,05E+01
	Std	8,07E-08	2,38E-10	1,79E-07	1,08E-06	3,47E-06	4,08E-04

Table 7 Configuration 3: Result of F1-23 benchmark functions

		Orginal	Henon map	Logistic map	Sine map	Tent map	Tinkerbell map
Category I: Unimodal benchmark functions							
F1	Ort	1,54E−02	1,04E−01	1,57E−02	4,37E−01	2,58E−02	4,19E+02
	Max	2,67E−02	1,44E−01	2,26E−02	6,13E−01	5,28E−01	7,33E+02
	Min	9,18E−03	3,75E−02	8,11E−03	2,78E−01	0,00E+00	2,53E+02
	Std	2,73E−03	1,81E−02	2,63E−03	8,00E−02	1,05E−01	1,07E+02
F2	Ort	5,47E+00	3,81E+00	5,67E+00	1,33E+01	1,51E+01	4,63E+01
	Max	1,38E+01	6,72E+00	2,28E+01	9,53E+01	1,08E+02	1,03E+02
	Min	1,24E+00	1,87E+00	1,99E+00	1,63E+00	1,70E+00	1,81E+01
	Std	2,55E+00	9,78E-01	4,07E+00	1,80E+01	2,43E+01	1,76E+01
F3	Ort	1,30E+00	3,75E+00	2,51E+00	6,49E+02	1,60E+02	3,44E+02
	Max	2,10E+00	5,49E+00	3,97E+00	8,91E+02	3,11E+02	6,75E+02
	Min	5,66E−01	1,86E+00	1,38E+00	5,06E+02	8,92E+01	1,06E+02
	Std	2,87E−01	7,57E−01	4,57E−01	6,42E+01	4,61E+01	1,18E+02
F4	Ort	1,49E+01	1,03E+01	1,47E+01	1,74E+01	1,74E+01	2,89E+01
	Max	1,77E+01	1,30E+01	1,72E+01	1,94E+01	2,04E+01	3,77E+01
	Min	9,67E+00	6,42E+00	1,20E+01	1,57E+01	1,53E+01	1,93E+01
	Std	1,50E+00	1,14E+00	1,15E+00	7,52E-01	8,75E-01	3,88E+00
F5	Ort	3,92E+01	6,97E+01	3,77E+01	7,89E+01	7,68E+01	1,39E+04
	Max	6,46E+01	1,02E+02	4,91E+01	1,15E+02	1,25E+02	4,11E+04
	Min	3,31E+01	4,62E+01	3,11E+01	4,83E+01	5,03E+01	4,36E+03
	Std	4,39E+00	1,24E+01	3,39E+00	1,38E+01	1,37E+01	6,32E+03
F6	Ort	1,55E−02	1,04E−01	1,60E−02	4,42E−01	4,25E−01	1,95E+02
	Max	2,21E−02	1,38E−01	2,24E−02	7,27E−01	8,76E−01	3,27E+02
	Min	6,98E−03	5,82E−02	1,06E−02	2,62E−01	2,83E−01	5,32E+01
	Std	3,19E−03	1,77E−02	2,40E−03	7,69E−02	1,04E−01	4,71E+01
F7	Ort	9,51E−02	4,30E−02	9,67E−02	5,90E−01	5,01E−01	3,17E−01
	Max	1,54E−01	8,04E−02	1,54E−01	7,18E−01	7,09E−01	5,27E−01
	Min	4,41E−02	1,68E−02	3,99E−02	4,48E−01	2,43E−01	1,37E−01
	Std	2,19E−02	1,21E−02	2,32E−02	5,08E−02	9,89E−02	8,30E−02
Category II: multimodal benchmark functions							
F8	Ort	−9,01E+03	−9,11E+03	−9,04E+03	−9,12E+03	−9,15E+03	−8,57E+03
	Max	−8,65E+03	−8,71E+03	−8,75E+03	−8,85E+03	−8,88E+03	−7,45E+03
	Min	−9,47E+03	−9,86E+03	−9,35E+03	−9,70E+03	−9,47E+03	−1,22E+04
	Std	1,52E+02	1,89E+02	1,28E+02	1,43E+02	1,42E+02	1,23E+03
F9	Ort	1,02E+02	8,86E+01	9,77E+01	9,42E+01	9,33E+01	1,58E+02
	Max	1,17E+02	1,13E+02	1,14E+02	1,13E+02	1,09E+02	1,89E+02
	Min	8,28E+01	6,31E+01	8,05E+01	7,73E+01	7,29E+01	1,16E+02
	Std	7,33E+00	1,04E+01	6,43E+00	6,02E+00	6,48E+00	1,74E+01
F10	Ort	1,06E+01	5,03E+00	1,18E+01	1,91E+01	1,90E+01	7,79E+00
	Max	1,56E+01	8,23E+00	1,85E+01	1,96E+01	1,95E+01	9,87E+00
	Min	6,28E+00	2,59E+00	8,84E+00	1,78E+01	1,39E+01	5,33E+00
	Std	2,16E+00	1,16E+00	1,81E+00	3,16E-01	8,25E-01	9,39E−01
F11	Ort	7,06E−02	2,27E−01	6,89E−02	4,16E−01	4,43E−01	2,75E+00
	Max	1,07E−01	2,98E−01	9,46E−02	6,01E−01	6,79E−01	3,86E+00
	Min	5,03E−02	1,52E−01	4,50E−02	2,86E−01	3,08E−01	1,71E+00
	Std	1,21E−02	3,21E−02	9,70E−03	5,37E−02	6,47E−02	4,16E−01
F12	Ort	4,11E+00	1,36E+00	3,86E+00	4,57E+00	4,57E+00	1,92E+01
	Max	5,19E+00	2,19E+00	5,09E+00	5,33E+00	5,59E+00	2,99E+01

Table 7 (continued)

		Orginal	Henon map	Logistic map	Sine map	Tent map	Tinkerbell map
	Min	1,55E+00	6,21E−01	2,57E+00	3,55E+00	3,31E+00	1,14E+01
	Std	5,71E−01	3,96E−01	4,88E−01	3,97E−01	4,62E−01	4,65E+00
F13	Ort	2,87E+00	2,62E+00	2,57E+00	1,55E+01	1,43E+01	1,85E+02
	Max	7,25E+00	4,09E+00	5,80E+00	2,10E+01	1,89E+01	2,93E+03
	Min	9,12E−01	1,50E+00	1,04E+00	1,04E+01	6,98E+00	2,99E+01
	Std	1,05E+00	5,91E-01	1,01E+00	1,91E+00	2,26E+00	3,32E+02
Category III: fix dimension multimodal benchmark functions							
F14	Ort	9,98E−01	9,98E−01	9,98E−01	9,98E−01	9,98E−01	9,98E−01
	Max	9,98E−01	9,98E−01	9,98E−01	9,98E−01	9,98E−01	9,98E−01
	Min	9,98E−01	9,98E−01	9,98E−01	9,98E−01	9,98E−01	9,98E−01
	Std	1,76E−15	1,23E−15	6,03E−15	4,68E−13	6,67E−11	1,04E−11
F15	Ort	3,11E−04	3,07E−04	3,15E−04	5,93E−04	5,84E−04	4,61E−04
	Max	3,45E−04	3,07E−04	4,08E−04	8,24E−04	7,35E−04	6,57E−04
	Min	3,08E−04	3,07E−04	3,08E−04	3,17E−04	3,35E−04	3,09E−04
	Std	5,85E−06	6,93E−13	1,38E−05	1,04E−04	8,94E−05	7,91E−05
F16	Ort	−1,03E+00	−1,03E+00	−1,03E+00	−1,03E+00	−1,03E+00	−1,03E+00
	Max	−1,03E+00	−1,03E+00	−1,03E+00	−1,03E+00	−1,03E+00	−1,03E+00
	Min	−1,03E+00	−1,03E+00	−1,03E+00	−1,03E+00	−1,03E+00	−1,03E+00
	Std	1,33E−15	1,56E−15	1,32E−15	2,30E−15	3,99E−15	7,21E−09
F17	Ort	3,98E−01	3,98E−01	3,98E−01	3,98E−01	3,98E−01	3,98E−01
	Max	3,98E−01	3,98E−01	3,98E−01	3,98E−01	3,98E−01	3,98E−01
	Min	3,98E−01	3,98E−01	3,98E−01	3,98E−01	3,98E−01	3,98E−01
	Std	1,06E−15	1,04E−15	1,07E−15	5,15E−15	2,06E−15	4,84E−08
F18	Ort	3,00E+00	3,00E+00	3,00E+00	3,00E+00	3,00E+00	3,00E+00
	Max	3,00E+00	3,00E+00	3,00E+00	3,00E+00	3,00E+00	3,00E+00
	Min	3,00E+00	3,00E+00	3,00E+00	3,00E+00	3,00E+00	3,00E+00
	Std	2,57E−15	1,01E−15	4,53E−15	3,40E−12	4,98E−12	1,86E−08
F19	Ort	−3,86E+00	−3,86E+00	−3,86E+00	−3,86E+00	−3,86E+00	−3,86E+00
	Max	−3,86E+00	−3,86E+00	−3,86E+00	−3,86E+00	−3,86E+00	−3,86E+00
	Min	−3,86E+00	−3,86E+00	−3,86E+00	−3,86E+00	−3,86E+00	−3,86E+00
	Std	6,86E−15	6,25E−15	6,23E−15	1,57E−12	1,30E−12	2,01E−08
F20	Ort	-3,32E+00	−3,32E+00	−3,32E+00	−3,32E+00	−3,32E+00	−3,32E+00
	Max	−3,32E+00	−3,32E+00	−3,32E+00	−3,32E+00	−3,32E+00	−3,32E+00
	Min	−3,32E+00	−3,32E+00	−3,32E+00	−3,32E+00	−3,32E+00	−3,32E+00
	Std	3,91E−12	1,52E−11	3,58E−12	1,85E−09	8,68E−10	2,74E−04
F21	Ort	−1,02E+01	−1,02E+01	−1,02E+01	−1,02E+01	−1,02E+01	−1,02E+01
	Max	−1,02E+01	−1,02E+01	−1,02E+01	−1,02E+01	−1,02E+01	−1,02E+01
	Min	−1,02E+01	−1,02E+01	−1,02E+01	−1,02E+01	−1,02E+01	−1,02E+01
	Std	3,52E−11	1,35E−13	4,58E−11	5,32E−09	4,56E−09	2,17E−05
F22	Ort	−1,04E+01	−1,04E+01	−1,04E+01	−1,04E+01	−1,04E+01	−1,04E+01
	Max	-1,04E+01	-1,04E+01	-1,04E+01	-1,04E+01	-1,04E+01	-1,04E+01
	Min	-1,04E+01	-1,04E+01	-1,04E+01	-1,04E+01	-1,04E+01	-1,04E+01
	Std	5,37E-11	3,49E-13	1,05E-10	5,81E-09	5,71E-09	3,49E-05
F23	Ort	−1,05E+01	−1,05E+01	−1,05E+01	−1,05E+01	−1,05E+01	−1,05E+01
	Max	−1,05E+01	−1,05E+01	−1,05E+01	−1,05E+01	−1,05E+01	−1,05E+01
	Min	−1,05E+01	−1,05E+01	−1,05E+01	−1,05E+01	−1,05E+01	−1,05E+01
	Std	3,50E−10	2,56E−12	3,52E−10	9,74E−09	8,39E−09	4,67E−05

Table 8 Number of best for each result of Configurataion 1-3 for benchmark functions

Configuration 1: result of F1-23 benchmark functions						
	Orginal	Henon map	Logistic map	Sine map	Tent map	Tinkerbell map
Ort	4	17	0	0	2	0
Max	5	16	1	0	1	0
Min	3	17	1	0	0	2
Std	4	8	3	5	3	0
Configuration 2: result of F1-23 benchmark functions						
	Orginal	Henon map	Logistic map	Sine map	Tent map	Tinkerbell map
Ort	2	17	4	0	0	0
Max	2	16	4	1	0	0
Min	5	16	3	0	0	1
Std	5	13	3	2	0	0
Configuration 3: result of F1-23 benchmark functions						
	Orginal	Henon map	Logistic map	Sine map	Tent map	Tinkerbell map
Ort	7	14	4	0	1	0
Max	4	14	3	0	2	0
Min	8	14	4	1	2	1
Std	1	11	8	3	0	0

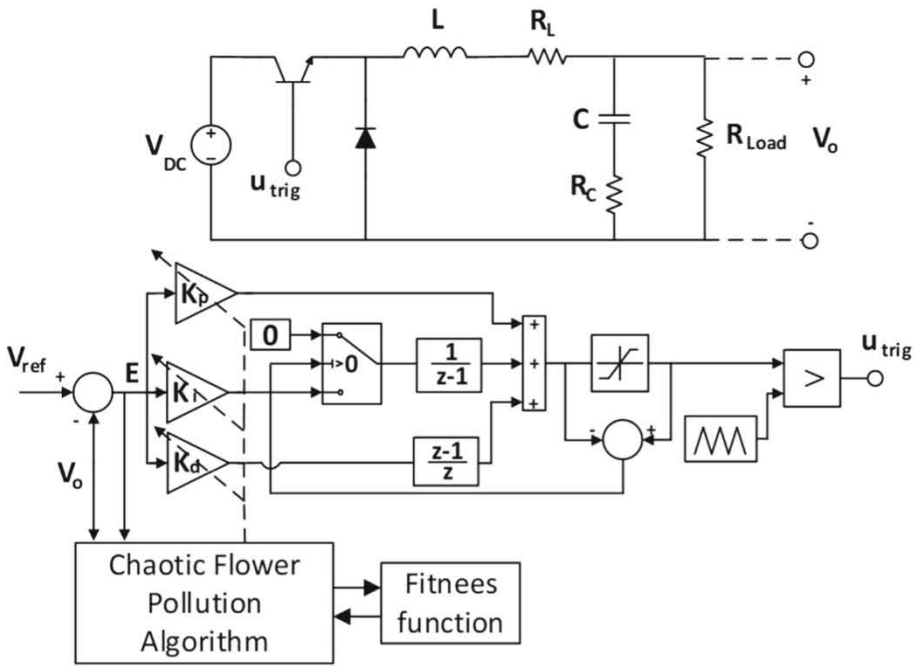

Fig. 3 PID design optimization for Buck Converter using Chaotic-FPA

Table 9 Flower Pollution Algorithm Parameters for Buck Converter

Parameter name	Parameter value
Population size	100
Probabilty switch	0.8
Iteration number	2000

tion, the system responses of these studies are given in Fig. 4.

The studies with whale optimization and firefly algorithms found in the literature show steady-state error. The cause of this error is due to their linearization of the system by only one point. The change of the system model between the initial state and the state in which it will operate is ignored. This result is obtained from the plant-model mismatch that could be ignored in many studies [20–22]. It is the integrator that will compensate this

Table 10 Statistical Results of Henon Based Chaotic FPA

Fitness function	Minimum error	Maximum error	Average error	Standart deviation	Times
ISE	0.7775	0.7841	0.7783	0.0020	30

Table 11 PID Parameters and Performance Results for Buck Converter

	Kp	Ki	Kd	ISE
Chotic flower pollution algorithm [proposed]	3.0458	1.4489	0.0001	0.7772
Firefly algorithm	51.59	56.88	0	0.8022
Whale optimization algorithm	36.1219	5.7947	0.00947	0.8275

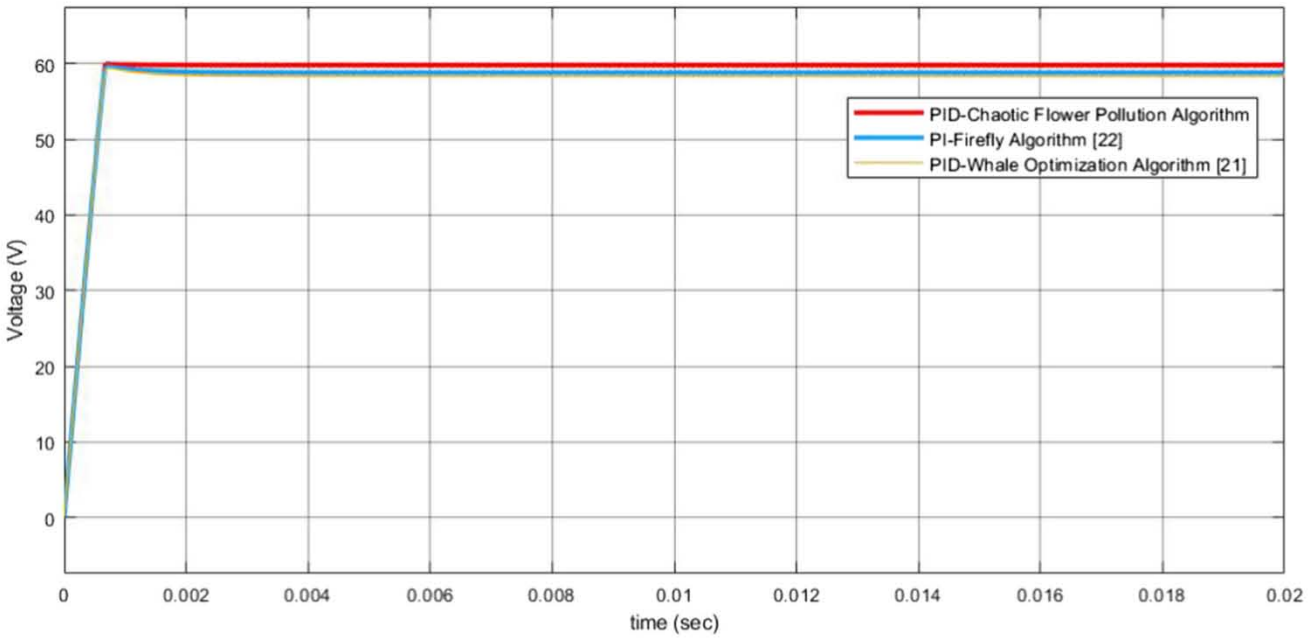

Fig. 4 PID Performance comparison for buck converter using various Meta-heuristic algorithm

mistmatch. It will cause the error to converge to zero in the steady state. In this study, the error value obtained from objective function was achieved by running the system on Matlab Simulink and since the controller was designed according to the obtained error value, the controller parameters were determined through the model that represents the actual system. Therefore, the results obtained with the Henon Based Chaotic-FPA, which is successful in the global search for the Buck Converter, were more successful than the controller designed with firefly algorithm and whale optimization [20, 21].

5 Conclusions

In this study, using the chaotic based flower pollination algorithm developed to control the buck converter increasing the performance of the system. To improve the global and local search capability of FPA, this paper proposes a hybridization method with Chaotic maps such as logistic, henon, tinkerbell, tent and sine maps to enhance the random searching capability of exploration and exploitation. In order to evaluate the effectiveness of the chaotic based FPA algorithms applied 23 different benchmark functions with different dimensions and characteristics. The performance of henon based FPA method is significantly better than other chaotic maps based FPA for all test functions. An antiwindup plugged PID controller with clamping structure was designed for buck converter by using the proposed henon based chaotic flower pollution algorithm. The henon based chaotic flower pollution algorithm was found to have a better performance when compared with the studies in the literature.

References

1. Bao, B., Zhang, X., Bao, H., Wu, P., Wu, Z., & Chen, M. (2019). Dynamical effects of memristive load on peak current mode buck-boost switching converter. *Chaos, Solitons & Fractals*, *122*, 69–79.
2. Alkrunz, M., et al. (2016). Design of discrete time controllers for the dc-dc boost converter. *Sakarya Üniversitesi Fen Bilimleri Enstitüsü Dergisi*, *20*(1), 75–82.
3. Yang, X.-S. (2010). *Nature-inspired metaheuristic algorithms*. United Kingdom: Luniver press.
4. X.-S. Yang (2013). Metaheuristic optimization: Nature-inspired algorithms and applications. In: *Artificial intelligence, evolutionary computing and metaheuristics*, Springer, Berlin pp. 405–420.
5. Talatahari, S., Azar, B. F., Sheikholeslami, R., & Gandomi, A. (2012). Imperialist competitive algorithm combined with chaos for global optimization. *Communications in Nonlinear Science and Numerical Simulation*, *17*(3), 1312–1319.
6. Gandomi, A. H., & Yang, X.-S. (2014). Chaotic bat algorithm. *Journal of Computational Science*, *5*(2), 224–232.
7. Batık, Z. G., Cimen, M. E., Karayel, D., & Boz, A. F. (2019). The chaos-based whale optimization algorithms global optimization. *Chaos Theory and Applications*, *1*(1), 51–63.
8. Çimen, M. E., & Boz, A. F. (2017). PSO, CS ve FA algoritmalarıyla ortak emiterli bjt'li yükselteç tasarımı. *Cumhuriyet Üniversitesi Fen-Edebiyat Fakültesi Fen Bilimleri Dergisi*, *38*(1), 119–130.
9. Çimen, M. E., & Boz, A. F. (2019). İkinci dereceden ölü zamanlı ve geri tepmeli sistem parametrelerinin, röle testi ve pso, cs, fa algoritmaları ile belirlenmesi. *Journal of the Faculty of Engineering & Architecture of Gazi University*, *34*(1), 461.
10. Liao, G.-C., & Tsao, T.-P. (2006). Application of a fuzzy neural network combined with a chaos genetic algorithm and simulated annealing to short-term load forecasting. *IEEE Transactions on Evolutionary Computation*, *10*(3), 330–340.
11. dos Santos Coelho, L., & de Andrade Bernert, D. L. (2009). An improved harmony search algorithm for synchronization of discrete-time chaotic systems. *Chaos, Solitons & Fractals*, *41*(5), 2526–2532.
12. Pluhacek, M., Senkerik, R., Zelinka, I., & Davendra, D. (2013) Chaos pso algorithm driven alternately by two different chaotic maps-an initial study. In: *(2013) IEEE congress on evolutionary computation*. (pp. 2444–2449). IEEE
13. Shayeghi, H., & Ghasemi, A. (2014). A modified artificial bee colony based on chaos theory for solving non-convex emission/economic dispatch. *Energy Conversion and Management*, *79*, 344–354.
14. Gong, W., & Wang, S.(2009). Chaos ant colony optimization and application. In: *2009 Fourth international conference on internet computing for science and engineering*, IEEE, pp. 301–303.
15. Gandomi, A. H., Yang, X.-S., Talatahari, S., & Alavi, A. H. (2013). Firefly algorithm with chaos. *Communications in Nonlinear Science and Numerical Simulation*, *18*(1), 89–98.
16. Bhowate, A., & Deogade, S. (2015). Comparison of pid tuning techniques for closed loop controller of dc-dc boost converter. *International Journal of Advances in Engineering & Technology*, *8*(1), 2064.
17. Sundareswaran, K., Kuruvinashetti, K., Hariprasad, B., Sankar, P., Nayak, P., & Vigneshkumar, V. (2014). Optimization of dual input buck converter control through genetic algorithm. *IFAC Proceedings Volumes*, *47*(1), 142–146.
18. Seo, K., & Choi, H.-H. (2012). Simple fuzzy pid controllers for dc-dc converters. *Journal of Electrical Engineering and Technology*, *7*(5), 724–729.
19. Swathy, M. K., Jantre, M. S., Jadhav, M. Y., Labde, M. S. M., & Kadam, M. P. (2018).Design and hardware implementation of closed loop buck converter using fuzzy logic controller. In: *2018 Second international conference on electronics, communication and aerospace technology (ICECA)*, IEEE, 2018, pp. 175–180.
20. Hekimoğu, B., Ekinci, S., & Kaya, S. (2019). Balina optimizasyon algoritması kullanılarak dada düşürücü dönüştürücünün optimum pid denetleyici tasarımı. In: *2018 International conference on artificial intelligence and data processing (IDAP)*
21. Mühürcü, G., Köse, E., Muhurcu, A., & Özdemir, M. (2018). Pi parameter optimization by fairly algorithm for optimal controlling of a buck converter's output state variable. *Sakarya Üniversitesi Fen Bilimleri Enstitüsü Dergisi*, *22*(5), 1267–1273.
22. Altinoz, O., & Erdem, H. (2010). Evaluation function comparison of particle swarm optimization for buck converter. In: *SPEEDAM 2010*, IEEE, pp. 798–802.
23. Gupta, A. K., Kumar, D., Reddy, B. M., & Samuel, P. (2017). BBBC based optimization of PI controller parameters for buck converter. In: *2017 Innovations in power and advanced computing technologies (i-PACT)* (pp. 1–6). IEEE.
24. Skvarenina, T. L. (2018). *The power electronics handbook*. Boca Raton: CRC Press.
25. Erdem, Z. (2009). *Maximum power point tracker*. Master Thesis, Electrical and Electronics Engineering, Sakarya University.
26. Erdem, Z. (2014). *Developing MDA formulations in PID design and DC-DC boost converter control for MPPT*. Phd Thesis, Electrical and Electronics Engineering, Sakarya University.
27. Kökçam, E. (2018). *Optimal control of output voltage of buck converter in the Matlab-simulink environment*. Master Thesis, Electrical and Electronics Engineering, Sakarya University.
28. Yang, X.-S. (2012). Flower pollination algorithm for global optimization. In: *International conference on unconventional computing and natural computation*, Springer, pp. 240–249.
29. Yang, X.-S., Karamanoglu, M., & He, X. (2014). Flower pollination algorithm: A novel approach for multiobjective optimization. *Engineering Optimization*, *46*(9), 1222–1237.
30. He, X.-S., Fan, Q.-W., Karamanoglu, M., Yang, X.-S. (2019) Comparison of constraint-handling techniques for metaheuristic optimization. In: *International conference on computational science*, Springer, pp. 357–366.

Murat Erhan Çimen received B.Sc. degree in Electrical and Electronics Engineering Department from Sakarya University and M.Sc. degree in Electrical and Electronics Engineering from the University of Sakarya University, Sakarya, Turkey. He has been with the Sakarya University of Applied Sciences, Turkey, Faculty of Technology, Electrical-Electronics Engineering Dept. as a Research Assisant. He performs research in the areas of control systems, engineering education, circuits, chaos, model predictive control and meta-heuristic algorithm.

Zeynep B. Garip received B.Sc. and M.Sc. degree in Electronics and Computer Education Department from Sakarya University, Sakarya, Turkey and Ph.D. degree in Mechatronics Engineering from the Sakarya University of Applied Sciences, Turkey. She has been with the Sakarya University of Applied Sciences, Turkey, Faculty of Technology, Computer Engineering Dept. as a Assisant Professor. She performs research in the areas of software development, mechatronics, robotic, chaos and meta-heuristic algorithm.

Ali Fuat Boz received B.Sc. degree in Electronics Education Department from Gazi University, Ankara, Turkey and Ph.D. degree in Control Engineering from the University of Sussex, Brighton, U.K. He has been with the Sakarya University of Applied Sciences, Turkey, Faculty of Technology, Electrical-Electronics Engineering Dept. as a Professor. He performs research in the areas of control systems, engineering education, circuits and systems.